International Journal of Research Studies in Science, Engineering and Technology
Volume 4, Issue 8, 2017, PP 20-27
ISSN : 2349-476X

Statistical Evaluation of Turbulence Variables for Flow Characteristics

O.P. Folorunso

Civil Engineering Department, Ekiti State University, Ado Ekiti. Nigeria.

***Corresponding Author:** O.P. Folorunso, Civil Engineering Department, Ekiti State University, Ado Ekiti. Nigeria.*

Received Date: 03-10-2017 ***Accepted Date: 07-10-2017*** ***Published Date:01-12-2017***

ABSTRACT

Flood management requires an established technique for effectiveness. Flow nature and the degree of flood risk can be determined by statistical methods. Because of the multi-scale physical phenomenon ofturbulent flow, such flow represents a significant parameter in flood hazard risk which exposes the environment to an undesirable event. Such flow can also be expressed using statistical methods as numerical index of a risk.This paper aims to determine flow characteristics and evaluation of open channel turbulence statistics in an idealized open channel. A high resolution turbulent measurements over the gravel and vegetated bed were made using the acoustic Doppler velocimeter (ADV), turbulent quantities were investigated through probability density distribution of turbulent velocities, turbulent intensities, autocorrelation and Reynold shear stresses. The results of this study will be useful to hydraulic engineers for river management and flood risks assessment and mitigation.

Keywords: *Turbulence, velocity, open channel, flood.*

INTRODUCTION

Majority of the flows that are of practical interest are mostly turbulent. The disturbances associated with changes in the fluid streamlines in turbulent conditions make such flows to become more complex. Turbulence is associated with vorticity, with the existence of random fluctuations in fluid flow, and at least on a small scale the flow is inherently unsteady.Turbulence is characterized by the time dependent chaotic behaviour seen in many fluid flows, this is due to the inertial of the fluid as a whole, and flows whose inertial effects tend to be small are laminar.

The random and unpredictable nature of turbulence requires the description of its motion through statistical measures because the instantaneous motions of turbulence are complicated to understand due to unexpected changes. A statistical description of turbulence involves a time average for stationary flows over multiple realizations to determine the mean occurrence. The velocity will typically be described as a time averaged value denoted by:

$$U = \frac{1}{T}\int_0^T udt \qquad (1)$$

Where, T is a time longer than the longest turbulent fluctuations in the flow. Example of time series record is shown in Figure (1).

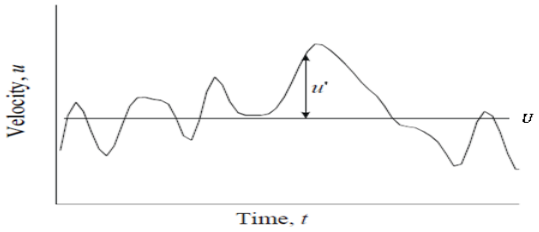

Figure1. *Schematic Example of Turbulence Time Series Record*

The magnitude of turbulence can be quantified using the turbulence intensity, i.e,

$$I_x, I_y, and\ I_z = \frac{\sigma_x}{U}, \frac{\sigma_y}{U}, and\ \frac{\sigma_z}{U} \qquad (2)$$

where $\boldsymbol{\sigma}$ is the standard deviation of the velocity fluctuation**.**

Probability Density Functions And Moments

A turbulent variable u at a given point and time can be described by the probability density function (PDF) $P(u)$:

$$\int_{-\infty}^{+\infty} P(u)du = 1 \qquad (3)$$

This is particularly important because, in the statistical theory of turbulence, the probability

density function provides a complete probabilistic description that permits the estimation and quantification of turbulent flow variables, for example, the tails of the pdf for flow variables have been reported to be influenced by the scale of eddy motions (Chu et al., 1996).

The skewness provides information about the asymmetry of the PDF given as:

$$Skewness\ (\mu_3) = \frac{u'^3}{(u'^2)^{3/2}} \quad (4)$$

where $u' = (u - U)$ is the turbulent fluctuating component.

The kurtosis characterizes the flatness of a PDF and is given by the expression:

$$kurtosis\ (\mu_4) = \frac{u'^4}{(u'^2)^2} \quad (5)$$

A time series with measurements clustered around the mean has low kurtosis and a time series by intermittent extreme events are characterized with high kurtosis.

Autocorrelation

The autocorrelation of a random process describes the correlation between values of the process at different points in time, as a function of the two times or of the time difference. It shows the correlation between the consecutive values of the time series. As a time resolved characteristics for the velocity components, it plays a major role in the analysis of the flow structures and especially for determining temporal and spatial flow scales. It can be computed by shifting the velocity records by a time delay $\tau = \Delta t$ equal to a multiple of the measurement interval, for each time delay, the autocorrelation can be obtained as:

$$R_{uu}(\tau = \Delta t) = \frac{\overline{u'(t)u'(t+\tau)}}{\sqrt{\overline{U^2}}.\sqrt{\overline{U^2}}} \quad (6)$$

where $R_{uu}(\mathrm{t})$ is the autocorrelation function, u' is the fluctuating part of the velocity, and τ is an increment of time delay (McConville, 2008). From the autocorrelation functions, the integral time scale (T_u) can be obtained by evaluating the area under the autocorrelation function which is normally stop when the function crosses the x-axis. Integrating numerically the autocorrelation function in Equation (6) to give integral time scale for streamwise velocity component as shown in Equation (7):

$$T_u = \int_0^t R_{uu}(t)dt \quad (7)$$

T_u yields a physical interpretation for turbulence, i.e., it is an indication of the average temporal scale of turbulent eddies (Lacey and Roy, 2008). Similarly, an integral length scale is an important parameter in characterizing the structure of turbulence. It measures the longest correlation distance between the flow velocities at two points in the flow field (Hinze, 1975). This can be obtained from Equation (8) as:

$$L_u = U\,T_u \quad (8)$$

MATERIALS AND METHODS

Measurements were conducted in 22mm long rectangular re-circulating flume of width $B = 614mm$with gravel and vegetated beds at the University of Birmingham (Figure 2). The channel is supplied from a constant head tank with a capacity of $45{,}500l$ in the laboratory roof. Twelve flow discharges (Q) were investigated with corresponding flow depths and water surface profiles to achieve a uniform flow condition for experimental conditions. The gravel region of the bed extends over $\left(0 \leq {}^{y}/_{B} \leq 0.5\right)$, and the vegetated region extends over $\left(0.5 \leq {}^{y}/_{B} \leq 1.0\right)$, where y is the lateral distance from the left hand side looking downstream and B is the channel width.

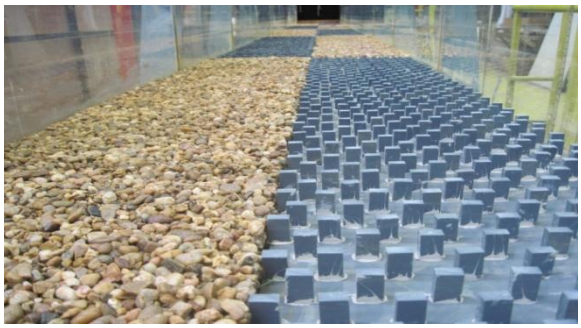

Figure2. *Rectangular Flow Channel*

Point Velocity Measurement

Velocity measurements were undertaken at the relevant cross sections, using a Nortek Vectrino acoustic Doppler velocimeter (ADV). Velocity data were collected in $10mm$ by $10mm$ grid spacing in the yz plane at the cross-sections with the first measurement taken at $10mm$ above the channel bed (within the sampling volume of the Vectrino). For each cross-section, a vertical profile of velocity data was collect. The variationof standard deviation of velocity$\boldsymbol{u}$ with Sample Length for optimum resolution is shown in Figure 3.

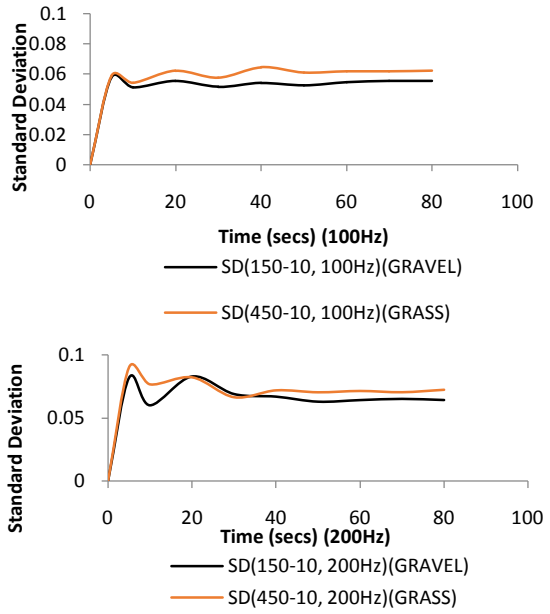

Figure3. *Variation of Standard Deviation of u with Sample Length*

Data filtering and Rotation

Data obtained from ADV is subject to uncertainties relating to the experimental conditions, e.g., probe alignment, measurement volume and signal aliasing. These uncertainties affect and compromise the accuracy of measurements. Misalignment of the probe can have a direct impact on the interpretation of velocity components and corresponding higher order statistics. Another source of error in ADV measurement is the Doppler noise. Doppler noise can be described as an error due to Doppler backscattering principle in calculating velocities (Lohrmann et al., 1994).

Data Processing

Spikes and outliers are created in the ADV data due to Doppler noise or poor signal to noise ratio as a result of inadequate particles in the flow to reflect the sound impulse signal. To process the ADV raw data, a filtering process was applied to remove spikes and noisy data in the time series signal. The ADV data can be filtered for low signal to noise ratio, low correlation coefficient of the velocity components and large deviation in velocity signal amplitude (Noise).

The "spikes" in the velocity signal were despiked using Phase-Space Threshold despiking algorithm proposed by Goring and Nikora (2002). The Phase-Space Threshold Method uses a phase-space plot in which the sampled velocity time series and their derivatives are plotted against each other to form points which are enclosed in an ellipsoid. The ellipsoid is defined by the sample mean and standard deviation and the points outside the ellipsoid are taken as spikes. The filtered signals by phase-space thresholds are shown in Figure 4. The signal is apparently good after applying phase space filtering method.The PDF of the filtered data are presented in Figure 5 for phase-space threshold values. It can be seen that the PDF of the phase-space filtered data is approximately Gaussian and normally distributed (Figure 5), Figure 6 illustrates the power spectral of the phase-space filtered velocity data, it can be seen that the resulting spectral distribution illustrates the different frequency ranges of the turbulent kinetic energy.

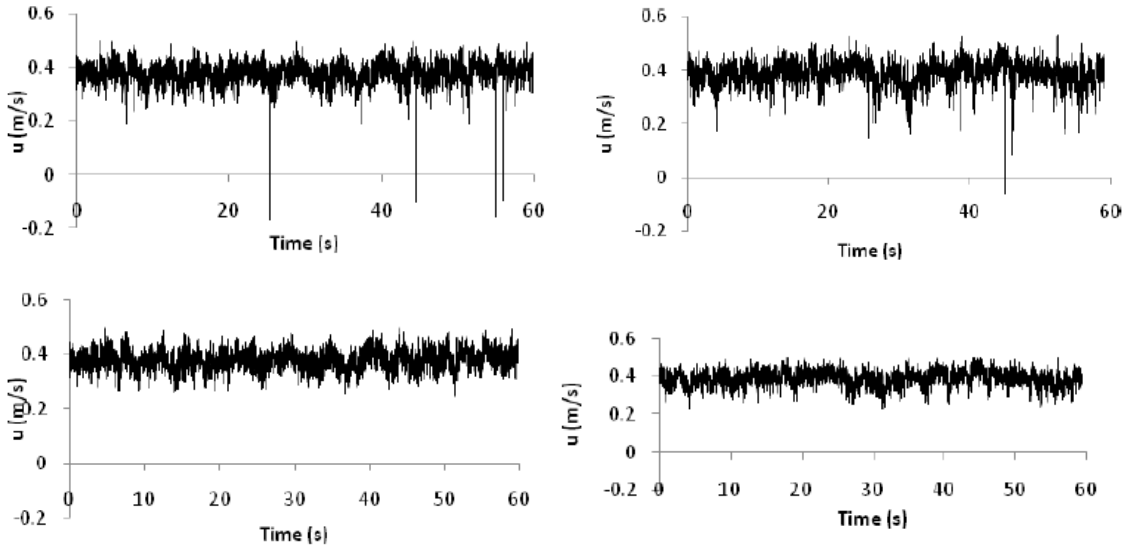

Figure4. *ADV Velocity Time Series Output signal (unfiltered) and the filtered signal using Phase-Space Threshold*

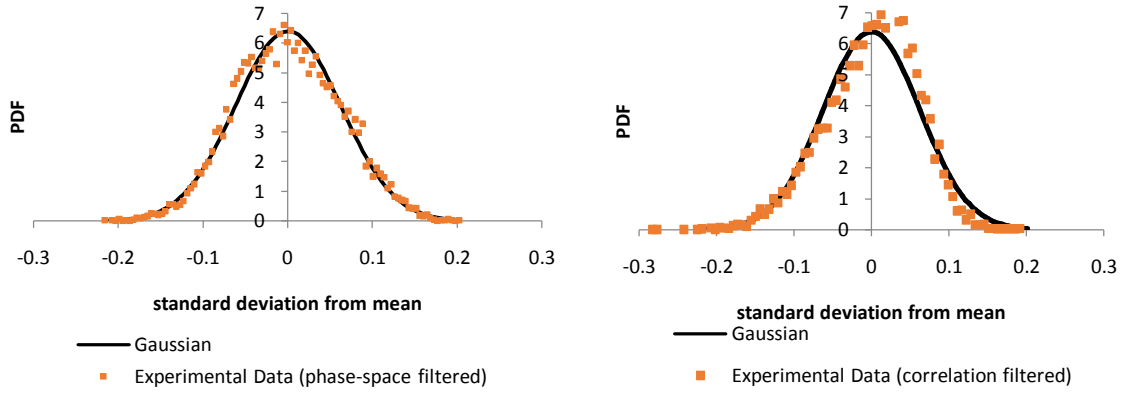

Figure5. *PDF Distribution* $\left(\frac{y}{B} = 0.5, EXPT1\right)$ *of (a) Filtered Data (phase-space); (b) Filtered Data (Correlation-signal to noise ratio)*

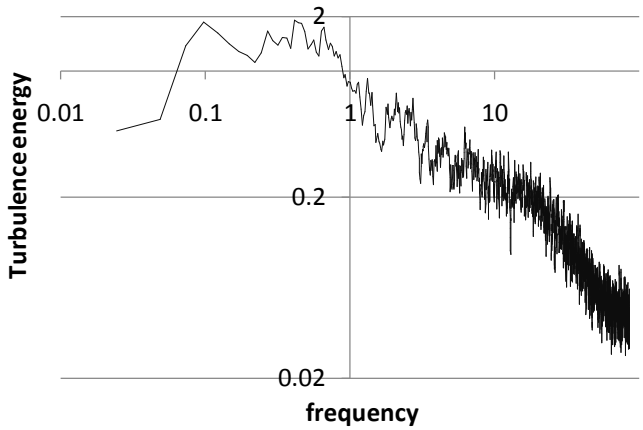

Figure6. *Power Spectral of the Filtered Data (phase-space)* $\left(\frac{y}{B} = 0.5, EXPT1\right)$

MEAN VELOCITY AND TURBULENCE CHARACTERISTICS

The logarithmic distribution of velocity is shown in Figure 7. The mean velocity vertical distributions correspond with the logarithmic profile thus indicating the flow to have characteristics akin to a two-dimensional structure.

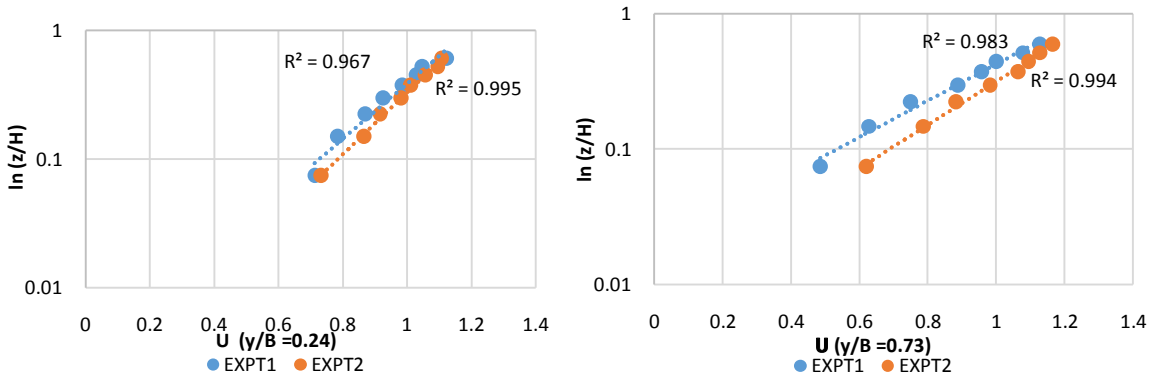

Figure7. *Logarithmic Distribution of the Mean Streamwise Velocity over Gravel and Vegetated region*

Figures 8illustrate the lateral distribution of normalized streamwise velocity $[U/(Q/A)]$ for the cross-sections, the distribution of the relative mean streamwise velocity appears to decelerate the near bed $\left({}^{z}/_{H} \leq 0.2\right)$. The flow is approximately symmetrical for $0.3 \leq {}^{z}/_{H} \leq 0.4$ across the section. Intuitively, the velocity maximum appears at the free surface within the

roughness boundary region and progressively reduces towards the channel bed.

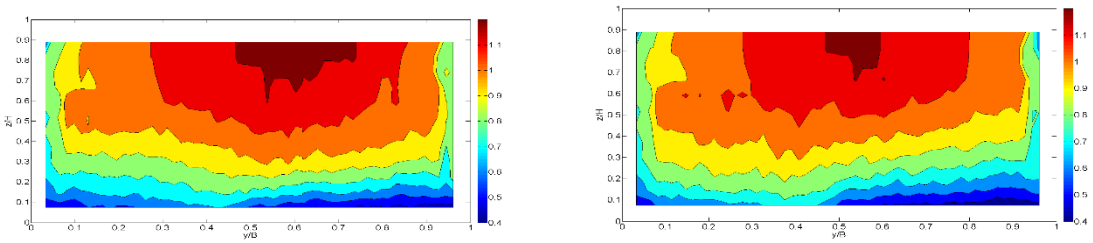

Figure8. *Lateral Mean Velocity Distribution*

Figures (9) show the vertical mean velocity (U) profiles for the cross sections. The figure confirms near bed $\left({}^{z}/_{H} \leq 0.2\right)$ deceleration as shown in Figure 8.

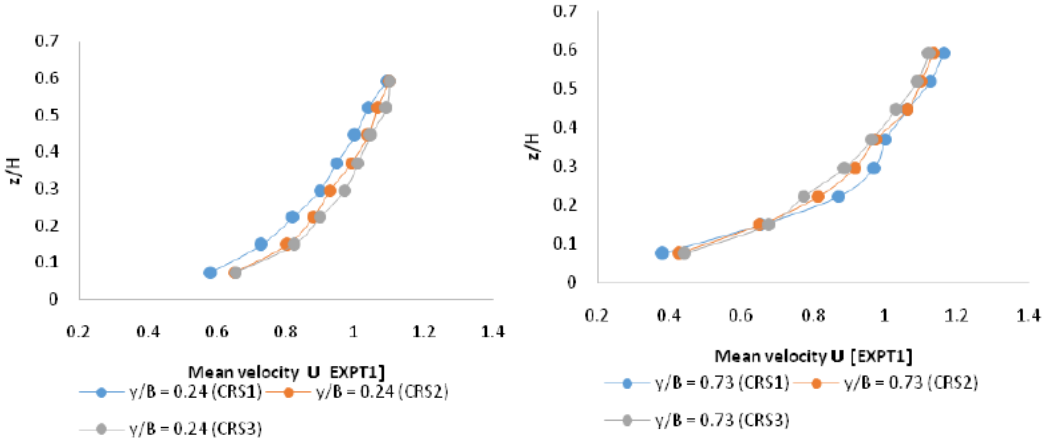

Figure9. *Vertical Distribution of Mean Velocity*

The vertical distributions of turbulent intensities at three locations are shown in Figure 10. As would be expected, due to velocity gradient and turbulence generation, the relative turbulence intensities reached the maximum values near the bed $\left({}^{z}/_{H} \leq 0.2\right)$ and in the region near the water surface $\left(0.4 \leq {}^{z}/_{H} \leq 0.6\right)$, the vertical turbulence intensity I_w is approximately constant. This is attributed to the free surface effect on the vertical turbulent fluctuation.

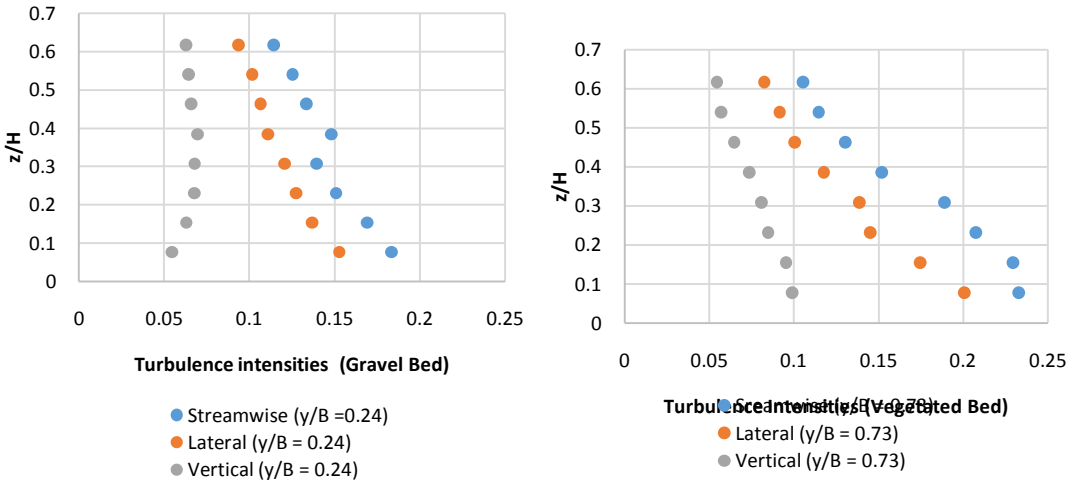

Figure10. *Vertical Distribution of the Relative Turbulence Intensities*

To characterize eddies transporting momentum in the flow, the streamwise temporal and length spatial scales of turbulent eddies are examined for efficient mass and momentum transfer and other transport processes in the flow. Evaluation of the length scale of eddies is preceded by

determining the time scale, to achieve this, autocorrelation function for streamewise velocity component $R_{(uu)}$ was used. The two-point correlation between the streamwise velocities fluctuations defined in Equation (6) is expressed as in Equation (9);

$$R_{(uu)}(\Delta t) = \frac{u'(t)u'(t+\Delta t)}{u'(t)u'(t)} \quad (9)$$

where u' represents the streamwise turbulent fluctuation, and Δt is the time lag.

The autocorrelation functions versus the time lag(Δt) given as $\Delta t = 0.005s$ (time interval between consecutive measurements) are shown in Figure 11for the near bed region of the flow. The decay rate of autocorrelation functions near bed is significant (Figure 11).The decay rate is approximately constant over the gravel section relative to vegetated bed (Figure 11); however the fluctuating velocities exhibit relative stronger turbulence connection in both experiments suggesting lower rate of turbulence dissipation. For the sake of clarity, autocorrelation functions are only presented for the near bed $\left(z/_H = 0.07\right)$ region as the upper region of the flow $\left(z/_H = 0.59\right)$ exhibited similar behaviour for the cross-sections.

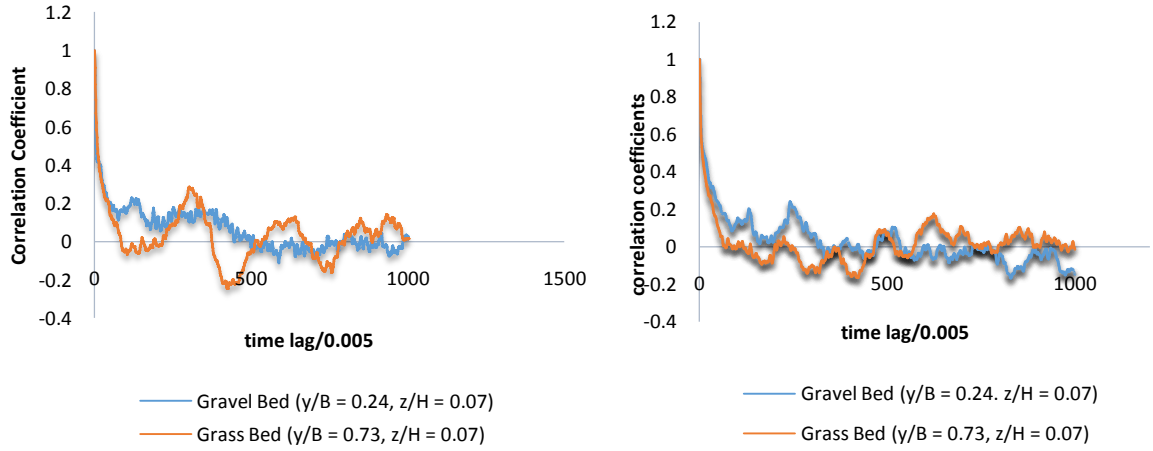

Figure111. *Autocorrelation Functions over Gravel and Grass Bed for Lower Region*

Using the autocorrelation functions of the streamwise velocity component in Equation (9), the integral time scale is obtained by evaluating the area under the autocorrelation function. Integrating numerically the autocorrelation functions using the expression in Equation (10):

$$T_u = \int_0^t R_{uu}(t)dt \quad (10)$$

Lacey and Roy (2008) described integral time scale T_u as an indication of the temporal scale of turbulent eddies. The temporal scale of eddies generally increases at the upper region of the flow for all the cross-sections reaching maximum value of 0.32s near the free surface over the vegetated bed. Lower magnitudes of time scale are recorded near bed, this is attributed to occurrence of shear and turbulence production near bed.

The integral length scale L_u corresponds to the size of fluctuating eddy motions that exists in turbulent flows, the streamwise integral length scale L_u is obtained from the streamwise integral time scale using Equation (11);

$$L_u = U\,T_u \quad (11)$$

Figure 12 illustrates vertical profiles of the normalized turbulent integral length scales. These figures demonstrate a general increase in depth with large variations around this trend. From Figure 12, eddies generated near the channel bed $\left(z/_H \leq 0.2\right)$ are much smaller, this is attributed to the boundary roughness and the burst (ejection) producing the turbulent eddies over the bed. The results however indicated that, the closer the eddies originate to the bed, the smaller their size in comparison to the upper region. This supports previous work by Yalin (1972) who observed the largest eddies did not occur near bed, however the experimental results demonstrate vortex stretching and the corresponding interaction thereof with other eddies as supported by the large variation (Figure 12). The finding is important because it

provides an approximation of eddy structure size in the flow.

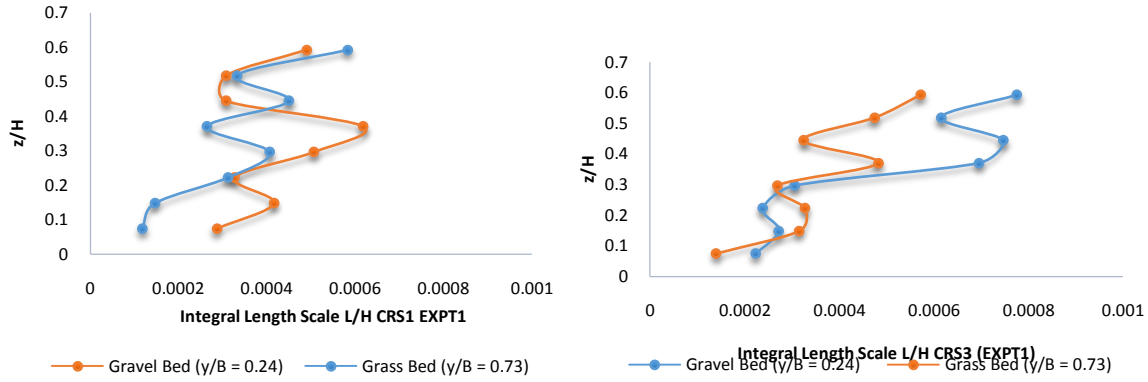

Figure12. *Vertical Profiles of Turbulent of Integral Length Scale*

Energy Power Spectral Density (EPSD) Distribution

The energy power spectrum was studied in order to explore which scales were mostly responsible for various level of turbulence. Figures 13 display power spectral $S(K_u)$, where K_u is the energy resulting from the streamwise velocity components defined for the near channel bed $(^{z}/_{H} = 0.07)$ at lateral positions $(^{y}/_{B} = 0.24\ (left),\ and\ ^{y}/_{B} = 0.73\ (right))$ over the gravel and vegetated bed respectively.

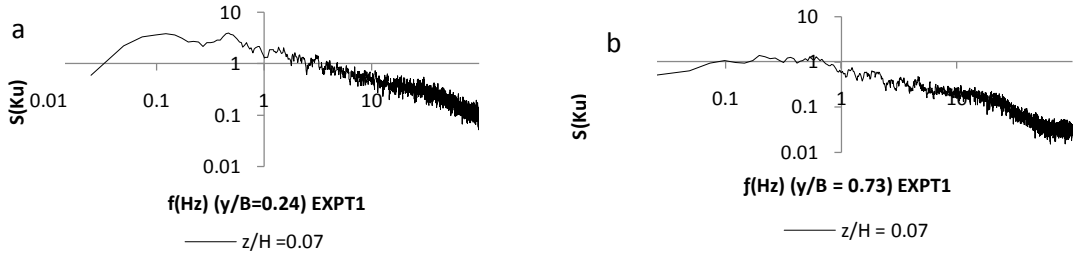

Figure13. *Energy Spectral Distribution near the Channel Bed* $(^{z}/_{H} = 0.07)$ *at* $(^{y}/_{B} = 0.24\ (left), and\ \ ^{y}/_{B} = 0.73\ (right))$

From Figure 13, it is evident that the peak frequencies f occurs within the range $0.3 - 0.5Hz$. Near the channel bed $(^{z}/_{H} = 0.07)$, the spectral distributions on the gravel section $(^{y}/_{B} = 0.24)$ obey the $^{-5}/_{3}$ power law with a wider occurrence of inertial subrange over a range of frequencies $1\ Hz < f < 60Hz$ (Figure 13). observed to be approximately constant as it does not decay significantly with frequency. It is shown from the figures that the inertia sub-range is wider near bed over the gravel section relative to vegetated section, and this becomes smaller as the distance from the bed increases to the upper region for both roughness sections.

Conclusion

The findings of the research analyzed statistically are highlighted as follows:

The results demonstrate that statistic can be used to determine the scale of turbulent velocities in open channel. It highlights the variation in casual mechanism pertaining to velocity fluctuations. The general trend in the integral length scale is an increase in depth with large variations around this trend, however, the large variation indicates vortex stretching and the corresponding interaction thereof with other eddies. It can be seen from the integral length scale that eddies generated near bed are smaller. This may initially suggest that the channel boundaries play a large part in the sizes of eddy formation, hence generating eddies with a length scale similar to the size of the boundary materials. However, it is possible to deduce that the eddy generated encounters the size of the roughness elements creating them.

References

[1] ANDERSON, J. 1995. Introduction to Computational Fluid Dynamics. McGraw Hill, Edition 6.

[2] BUFFING-BELANGER, T. & ROY, A. G. 2005. 1 min in the life of a river: Selecting the optimal record length for the measurement of turbulence in fluvial boundary layers Geomorph.,, 68, 77-94.

[3] CAROLLO, F. G., FERRO, V. & TERMINI, D. 2005. Analyzing turbulence intensity in gravel bed channels. Journal of Hydraulic Engineering, 131, 1050-1061.

[4] CEA, L., PUERTAS, J. & PENA, L. 2007. Velocity measurements on highly turbulent free surface flow using ADV. Experiments in Fluids 42, 333-348.

[5] CHOW, V. T. 1959. Open-Channel Hydraulics. McGraw-Hill Singapore.

[6] CHU, C. R., PARLANGE, M. B., KATUL, G. G. & ALBERTSON, J. D. 1996. Probability density functions of turbulent velocity and temperature surface layer. Water Resources Research, 32, 1681-1688.

[7] DANIEL, E., DOMBROSKI & JOHN, P. C. 2007. The accuracy of acoustic Doppler velocimetry measurements in turbulent boundary layer flows over a smooth bed. Limnol. Oceanogr.: Methods, 5, 23-33.

[8] DAVIDSON, P. A. 2004. Turbulence - an introduction for scientists and engineers. Oxford University Press.

[9] ELDER, J. W. 1954. The dispersion of marked fluid in turbulent shear flow. Cavendish Laboratory, University of Cambridge, 544-560.

[10] GORING, D. G. & NIKORA, V. I. 2002. Despiking acoustic Doppler velocimeter data. Journal of Hydraulic Engineering, 128, 117-126.

[11] HA, H. K., MAA, J. P.-Y., SHAO, Y. Y. & HOLLAND, C. W. 2009. Using ADV backscatter strength for measuring suspended cohesive sediment concentration. Continental Shelf Research, 29, 1310–1316.

[12] HAYWOOD, L. 1996. Airline Turbulence: Staying Safe in the Air. dspace.mit.edu.

[13] HINZE, J. O. 1975. Turbulence. McGraw-Hill series in mechanical engineering.

[14] HOFLAND, B. & BATTJES, J. 2006. Probability density of instantaneous drag forces and shear stresses on a bed. Journal of Hydraulic Engineering, 132, 1169-1175.

[15] JIMENEZ, J. 2004. Turbulent flows over rough walls. Fluid Mech, 36, 173-96.

[16] KAIMAL, J. C. & FINNIGAN, J. J. 1994. Atmospheric Boundary Layer Flow, . Oxford University Press.

[17] KNIGHT, D. W., MCGAHEY, C., LAMB, R. & SAMUELS, P. G. 2010. Practical Channel Hydraulics. London, CRC Press/Balkena, Taylor & Francis Group.

[18] LACEY, R. W. J. & ROY, A. G. 2008. Fine-scale characterization of the turbulent shear layer of an instream pebble cluster. Journal of Hydraulic Engineering, 137, 925-926.

[19] LANE, T., SHARMAN, R. D., TRIER, S. B., FOVELL, R. G. & WILLIAMS, J. K. 2012. Recent advances in the understanding of near-cloud turbulence. Advances in numerical modeling and new observations, 499-515.

[20] LOHRMANN, A., CABRERA, R. & KRAUS, N. C. 1994. Acoustic Doppler velocimeter (ADV) for Laboratory Use. Fundamentals and Advancements in Hydraulic Measurements and Experimentation. Buffalo, New York. ASCE, 351-365.

[21] MCLELLAND, S. J. & NICHOLAS, A. P. 2000. A new method for evaluating errors in high frequency ADV measurements. . Hydrological processes., 14, 351-366.

[22] NAKAGAWA, H., NEZU, I. & UEDA, H. 1975. Turbulence of Open channel flow over smooth and rough beds. Proceedings of JSCE, 241, 155-168.

[23] NEZU, I. & NAKAGAWA, H. 1993. Turbulence in open-channel flows,. Rotterdam, A.A. Balkema.

[24] NEZU, I. 1977. Turbulence intensities in open-channel flows. Journal of JSCE, 261, 67-76.

[25] NIKORA, V. I. & GORING, D. G. 1998. ADV Measurements of turbulence: can we improve their interpretation. Journal of Hydraulic Engineering, 124, 630-634.

[26] PRANDTL, L. 1952. Essentials of fluid dynamics.

[27] TENNEKES, H. & LUMLEY, J. L. 1972. A first course in turbulence. The MIT Press Cambridge, Massachusetts, and London, England.

[28] VOULGARIS, G. & TROWBRIDGE, J. H. 1998. Evaluation of the Acoustic Doppler Velocimeter (ADV) for Turbulence Measurements. J O U R N A L O F A T M O S P H E R I C A N D O C E A N I C T E C H N O L O G Y, 15, 272-289.

[29] YEN, B. C. 2002. Open channel flow resistance. Journal of Hydraulic Engineering, 128, 20-39.

Citation: *O. Folorunso, "Statistical Evaluation of Turbulence Variables for Flow Characteristics", International Journal of Research Studies in Science, Engineering and Technology, vol. 4, no. 8, pp. 20-27, 2017.*